Climate Variability in a Coupled GCM. Part II: The Indian Ocean and Monsoon

M. LATIF, A. STERL,* M. ASSENBAUM, M. M. JUNGE, AND E. MAIER-REIMER

Max-Planck-Institut für Meteorologie, Hamburg, Germany

(Manuscript received 23 February 1993, in final form 12 January 1994)

ABSTRACT

We have investigated the seasonal cycle and the interannual variability of the tropical Indian Ocean circulation and the Indian summer monsoon simulated by a coupled ocean–atmosphere general circulation model in a 26-year integration. Although the model exhibits significant climate drift, overall, the coupled GCM simulates realistically the seasonal changes in the tropical Indian Ocean and the onset and evolution of the Indian summer monsoon. The amplitudes of the seasonal changes, however, are underestimated.

The coupled GCM also simulates considerable interannual variability in the tropical Indian Ocean circulation, which is partly related to the El Niño/Southern Oscillation phenomenon and the associated changes in the Walker circulation. Changes in the surface wind stress appear to be crucial in forcing interannual variations in the Indian Ocean SST. As in the Pacific Ocean, the net surface heat flux acts as a negative feedback on the SST anomalies.

The interannual variability in monsoon rainfall, simulated by the coupled GCM, is only about half as strong as observed. The reason for this is that the simulated interannual variability in the Indian monsoon appears to be related to internal processes within the atmosphere only. In contrast, an investigation based on observations shows a clear lead–lag relationship between interannual variations in the monsoon rainfall and tropical Pacific SST anomalies. Furthermore, the atmospheric GCM also fails to reproduce this lead–lag relationship between monsoon rainfall and tropical Pacific SST when run in a stand-alone integration with observed SSTs prescribed during the period 1970–1988. These results indicate that important physical processes relating tropical Pacific SST to Indian monsoon rainfall are not adequately modeled in our atmospheric GCM. Monsoon rainfall predictions appear therefore premature.

1. Introduction

The climate system in the Indian Ocean/Asian region is characterized by rapid changes on seasonal timescales that are forced by the seasonal variations in the differential heating of the Indian Ocean and the adjacent Asian landmasses (Meehl 1992). This differential heating forces the monsoon circulation in the atmosphere that gives rise to the Indian summer monsoon rainfall. Also, the seasonal variations in the monsoon circulation drive characteristic circulation patterns in the Indian Ocean. Among those, the annual reversal of the Somali Current and the semiannual occurrence of an equatorial surface jet, the Wyrtki jet, are the most prominent representatives (Lighthill 1969; Wyrtki 1973).

The Indian Ocean/Asian region has attracted many modeling efforts. Reviews of Indian Ocean modeling can be found, for instance, in Knox and Anderson (1985), Knox (1987), and Luther (1987), whereas an overview of recent monsoon modeling activities focusing on the predictability of monsoon rainfall is given in a workshop report issued by the World Meteorological Organization (WMO 1992). However, although large-scale air–sea–land interactions are crucial in understanding the climate variability in this part of the world, most modeling studies were conducted using single component models prescribing boundary conditions from observations. Here, we describe the climate variability in the Indian Ocean/Asian region simulated by a coupled ocean–atmosphere general circulation model (CGCM). The CGCM, described in detail in Part I of this paper (Latif et al. 1993a, hereafter referred to as Part I), simulates realistically the climate variability in the tropical Pacific, in particular the El Niño/Southern Oscillation (ENSO) phenomenon, and was also applied successfully to ENSO predictions (Latif et al. 1993b).

Coupled modeling is a rapidly progressing field because of the large scientific and public interest in predictions of potential anthropogenic climate changes and natural climate variations. Both issues require a proper representation of both oceanic and atmospheric circulation. The tropical behavior of a large number

* Current affiliation: KNMI, Postbus 201, NL-3730 AE de Bilt, the Netherlands.

Corresponding author address: Dr. Mojib Latif, Max-Planck-Institut für Meteorologie, Bundesstrasse 55, 20146 Hamburg, Germany.

of coupled ocean–atmosphere general circulation models was described recently by Neelin et al. (1992). However, this study was restricted to the tropical Pacific because of the predominance of the ENSO phenomenon in the interannual variability of the tropical climate system. However, there are other important scientific questions related to the tropical climate system for which coupled models are needed. For instance, will the monsoon circulation and its typical rainfall patterns change in response to the increased abundance of greenhouse gases in the atmosphere? Or, can we predict the strength of next year's Indian summer monsoon or Sahel rainfall?

Before, however, we can answer these and other important questions related to the tropical climate system, we have to verify the coupled models since they generally suffer from climate drift even when the individual model components give realistic results when forced by observed boundary conditions. The intention behind this paper is along these lines. Our main focus here is whether our coupled GCM is able to reproduce the fundamental seasonal and interannual variations in the monsoon and in the Indian Ocean circulation. We also investigate the interactions between the monsoon and ENSO and address the issue of monsoon predictability.

So far, only a few coupled modeling studies exist that address these topics. Meehl (1989) investigated the results of his coupled ocean–atmosphere GCM in view of the importance of active ocean dynamics. However, climate drift due to the coarse ocean model resolution was significant in this coupled model so that the coupled GCM simulated a monsoon that was too weak, especially over eastern Asia. Barnett et al. (1989) studied the effect of anomalous Eurasian snow cover on regional and global climate. This study showed that the strength of the Indian summer monsoon is sensitive to anomalous snow cover over Eurasia, a result already suggested by the observational work by Hahn and Shukla (1976). Furthermore, they also found some evidence for an influence of anomalous snow cover on the ENSO cycle, but climate drift in that coupled model was also a serious problem so that this point could not be addressed adequately.

This paper is organized as follows: In section 2, we describe briefly the coupled model. Section 3 deals with the simulation of the annual cycle in both the ocean and the atmosphere, whereas the interannual variability is described in section 4. The main conclusions of this study are given in section 5.

2. Coupled model

Here, we give only a brief description of the coupled GCM (CGCM), since it was already described in more detail in Part I of this paper. The domain of the ocean GCM (OGCM) extends from 70°N to 70°S and all three oceans are included. The model, however, is dynamically active only in the region 30°N to 30°S. Outside this belt, the model state is relaxed to Levitus (1982) climatology by applying a Newtonian formulation. The horizontal resolution of the OGCM was chosen in such a way that equatorially trapped waves are well resolved with a meridional resolution of 0.5° in the region 10°N to 10°S. The meridional resolution decreases poleward and remains constant at 5° poleward of 30°. The zonal resolution is constant at 5°. In the vertical, we use 17 irregularly placed levels with 10 levels in the upper 300 m.

The atmospheric general circulation model (AGCM) is the Hamburg version of the European Centre For Medium-Range Weather Forecasts (ECMWF). It is a low-order spectral model that explicitly resolves waves up to zonal wavenumber 21 (T21). The nonlinear terms are calculated on a 64×32 Gaussian grid, which yields a horizontal resolution of about $5.6° \times 5.6°$. There are 19 levels in the vertical, defined on σ surfaces in the lower troposphere and on p surfaces in the upper troposphere and stratosphere. The model includes standard physics, such as a boundary layer parameterization and interactive clouds.

The two models have been coupled without applying any correction. They exchange information over all three oceans in the region 30°N to 30°S. Outside this region boundary values are prescribed from climatology. While the AGCM is driven with the SSTs simulated by the OGCM, the OGCM is forced by the momentum, heat, and freshwater fluxes simulated by the AGCM. The coupling interval is two hours. The CGCM is forced by seasonally varying insolation. Initial conditions for the OGCM were obtained from an uncoupled 29-year control run with seasonally varying boundary forcing, whereas those for the AGCM were taken from an analysis of 1 January 1988. The coupled integration starts at 1 January and is continued for 26 years.

3. Annual cycle

Long-term monthly averages were computed from the 26-year run in order to investigate the annual cycle. We first describe the January and July climatologies simulated by the coupled model and compare them with observations. We restrict ourselves to these two months because they are most important with respect to the monsoon and the Indian Ocean circulation. The level of correspondence between the coupled model simulation and observations in these two months is fairly typical for the whole year (see Fig. 7).

a. January maps

The observations show an almost zonal structure in sea surface temperature in January (Fig. 1a). The

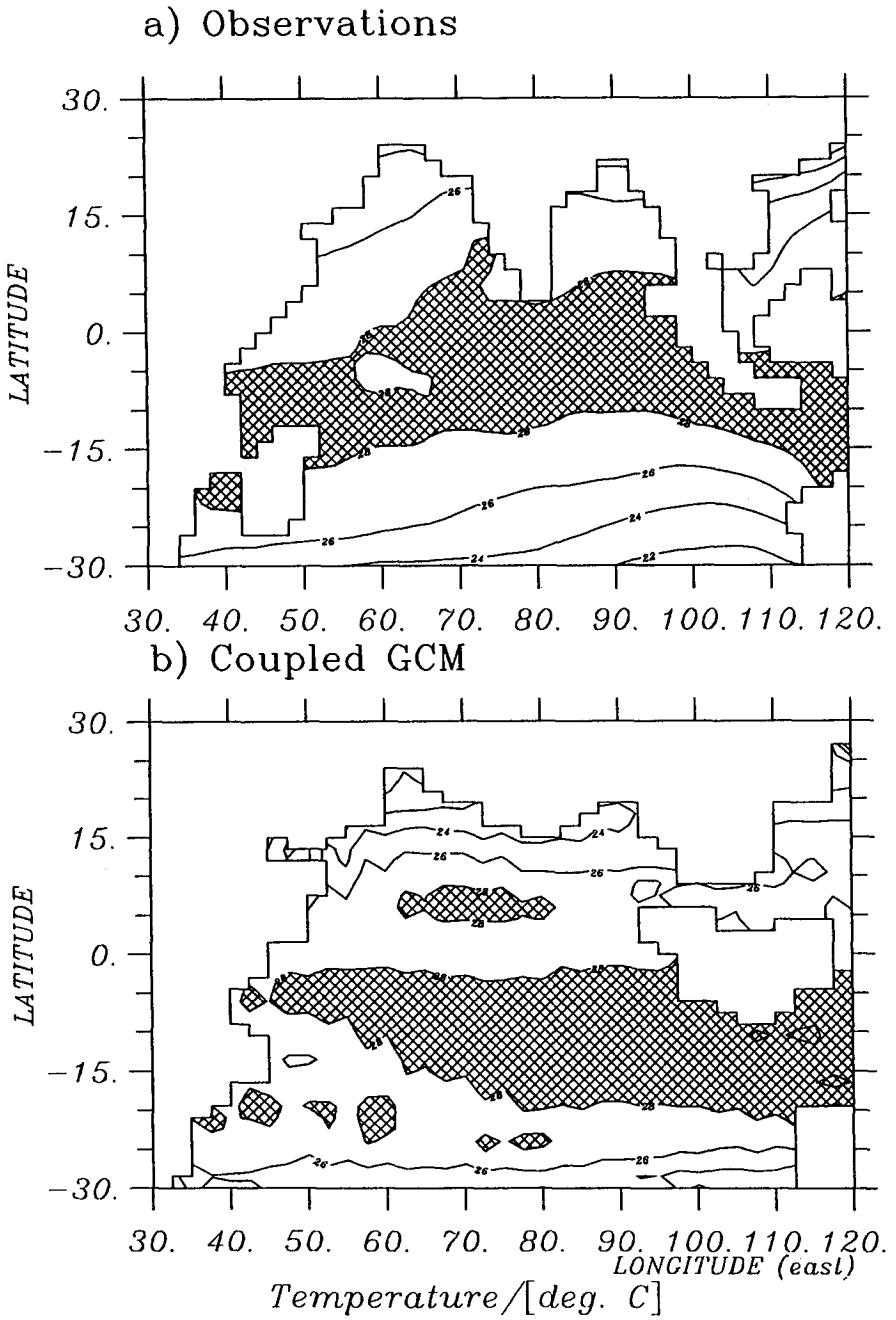

FIG. 1. (a) Climatological January SST (°C) after Levitus (1982); (b) long-term mean January SST (°C) derived from the 26-year run with the CGCM. Shading indicates areas with SST ≥ 28°C.

warmest surface waters are located predominantly south of the equator and extend to about 15°S. Typical temperatures in the warm pool are in the range from 28° to 29°C. Poleward of 15°S the SST decreases and attains a value of about 20°C near 30°S. North of the equator, the SST pattern is fairly flat and attains values less than 24°C in small regions near the continents only. The CGCM simulates the basic features of the January SST pattern (Fig. 1b). The warm pool, however, extends too far south, and the SST south of 20°C is typically 2°C warmer than observed. This systematic bias of the CGCM is probably due to an interaction of

the incoming solar radiation and the Richardson number–dependent vertical mixing scheme in the ocean. As already described in Part I, the solar radiation stabilizes the upper ocean layers in the subtropical regions, which damps the vertical mixing of heat, leading to a shallow warm surface layer. The inclusion of a solar radiation penetration scheme in our ocean model might reduce this problem. North of the equator, the coupled model tends to simulate temperatures too cold in the Red and Arabian Seas and south of India.

The map of climatological January wind stress as derived from the Hellermann and Rosenstein (1983) dataset (Fig. 2a) is dominated by the northeast monsoon and the southwest trades, which converge near 10°S. The CGCM simulates a similar wind stress pattern (Fig. 2b). The model, however, simulates the convergence zone about ten degrees too far south so that it is located near 20°S. This model deficiency is probably related to the SST error in the Southern Hemisphere described above (Fig. 1).

The climatological January rainfall (Figs. 3a and 3b) attains its maximum in the intertropical convergence zone (ITCZ) extending from southern Africa to the equatorial eastern Indian and western Pacific Ocean. This feature is evident in the two available climatologies (Jäger 1976; Legates and Willmott 1990), which are both shown in Fig. 3 to provide an indication of the uncertainty in climatological rainfall estimates. Maximum rainfall within the ITCZ is of the order of 8 mm/day. The CGCM fails to reproduce the correct orientation of the ITCZ (Fig. 3c) and simulates it as a zonal band located near 15°S. Furthermore, rainfall within the ITCZ is overestimated by the model, with typically 20% more rainfall than in the observations. The reason for the excessive zonal structure of the model ITCZ is that the western equatorial Pacific is too cold in the CGCM, which forces the convection to regions off the equator (see Part I, Fig. 2). In the Northern Hemisphere the CGCM does not show any significant rainfall in agreement with the observations.

b. June maps

The warm surface waters follow basically the movement of the sun. During April, the coupled model simulates the high equatorial SSTs ($\geq$28°C) in the region 15°N to 15°S (not shown). The climatological June SST is characterized by uniformly warm surface waters north of the equator and a moderate meridional SST gradient in the Southern Hemisphere (Fig. 4a). The CGCM simulates a similar SST pattern (Fig. 4b). The most obvious difference between the coupled model simulation and the observations is a dipole pattern in the model SST, which consists of too cold temperatures south of India and too warm SSTs in the Bay of Bengal. This model error, however, due to its small spatial extent, is unlikely to affect the large-scale atmospheric circulation.

This is confirmed by the comparison of the observed with the simulated June surface stress (Fig. 5). The CGCM simulates a realistic wind stress pattern (Fig. 5b) with a pronounced southeast monsoon, which gives rise to an intense Indian summer monsoon rainfall (Fig. 6). However, the CGCM does not reproduce the spatial details in the observed rainfall pattern, such as the minimum in rainfall over western India in the lee of the Ghats. The T21 resolution of our atmosphere model is certainly too coarse to adequately resolve small-scale orographic features that lead to the observed regional rainfall pattern. A minimum in monsoon rainfall over western India, however, is found in an extended-range integration with a T42 version of our atmosphere model forced by climatological SST (Arpe 1994, personal communication). This suggests that the inability of our model to reproduce the observed rainfall pattern is due mainly to the coarse resolution of our atmosphere model.

During the monsoon season, the model rainfall propagates northeastward (not shown), in agreement with observations. The amount of rainfall and mean onset date of the model monsoon is also in good agreement with observations (Tables 1 and 2). Overall, the CGCM simulates a realistic mean monsoon given the coarse resolution of the atmosphere model (see also Fig. 9).

c. Temporal evolution

We compare first the annual cycle in SST averaged over three equatorial boxes (Fig. 7). The coupled model simulation is in reasonable agreement with the climatology of Levitus (1982). In the equatorial western Indian Ocean the model simulates temperatures slightly too warm, but the phase of the annual cycle is reproduced reasonably well. In the central and eastern equatorial Indian Ocean, temperatures are simulated slightly too cold and the model overestimates the semiannual component in SST. This latter deficiency is particularly obvious in the eastern Indian Ocean during boreal fall when SSTs are simulated about 1.5°C too cold.

The Indian Ocean circulation is characterized by rapid changes on seasonal timescales. These changes arise from large-scale air–sea–land interactions and are therefore important in verifying coupled models. One of the most interesting phenomenon of the Indian Ocean circulation is the twice yearly occurrence of the Wyrtki jet (Wyrtki 1973), a strong eastward flowing surface current at the equator. Although the coupled GCM simulates the two occurrences of the Wyrtki jet, the model simulation is strongly biased towards westward currents (Fig. 8). Typical current speeds derived from observations are of the order of 60–80 cm s^{-1} (Reverdin 1987, Fig. 8a), whereas the model jet attains only speeds up to about 20 cm s^{-1} during spring (Fig. 8b). Furthermore, the second occurrence of the Wyrtki

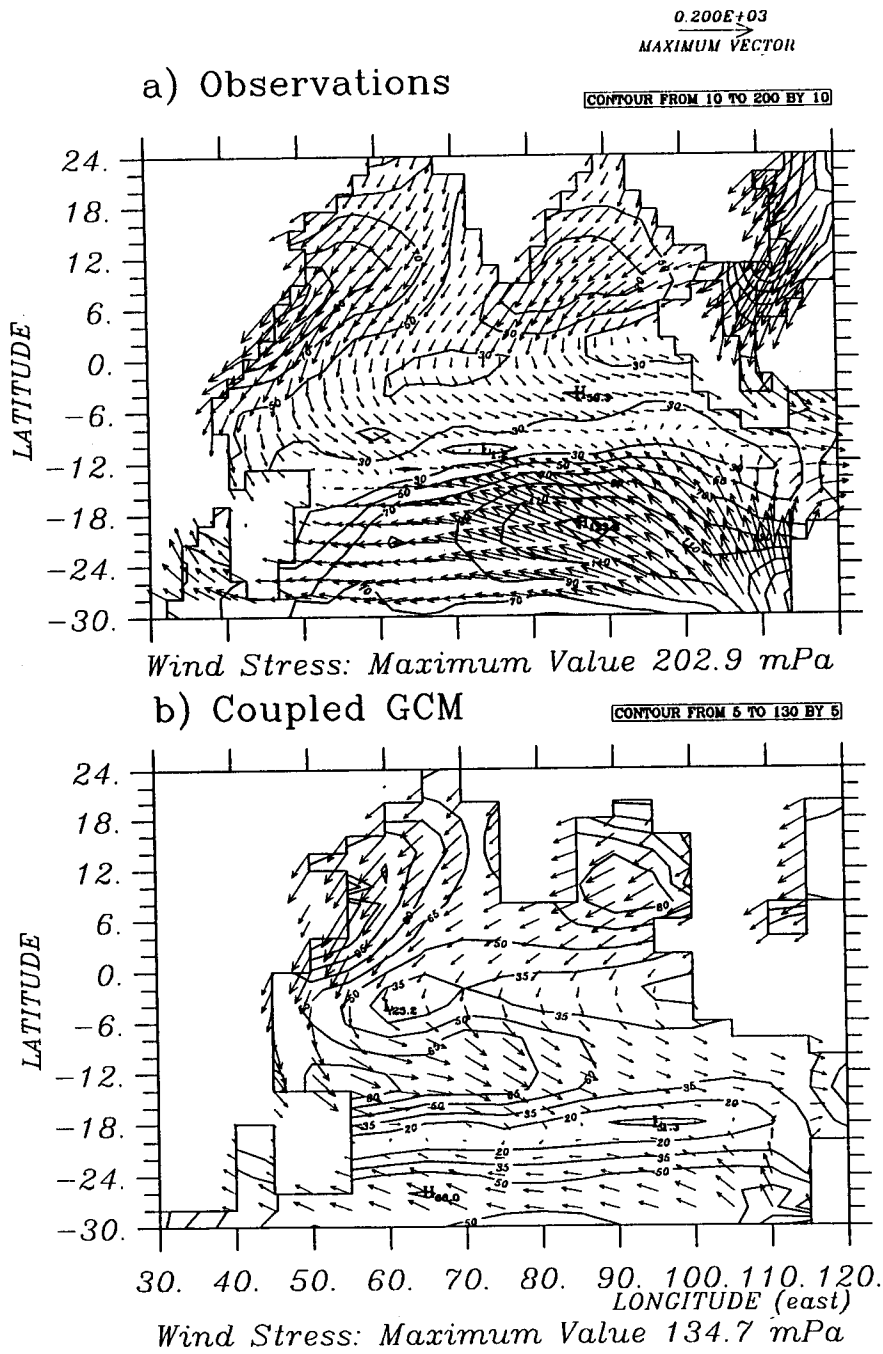

FIG. 2. (a) Climatological January surface wind stress (m Pa) after Hellermann and Rosenstein (1983); (b) long-term mean January surface wind stress (m Pa) derived from the 26-year run with the CGCM.

jet in fall is simulated by the model only in the far eastern Indian Ocean. However, although the model shows a strong bias towards westward currents at the equator, it simulates in agreement with the observations at least a strong semiannual cycle and westward phase propagation at the equator.

The surface current variability in the western Indian Ocean is dominated by the annual reversal of the Somali Current (Lighthill 1969). The CGCM simulates this feature of the Indian Ocean circulation reasonably well (Fig. 9). However, due to the coarse zonal model resolution (5°) boundary currents are not well resolved

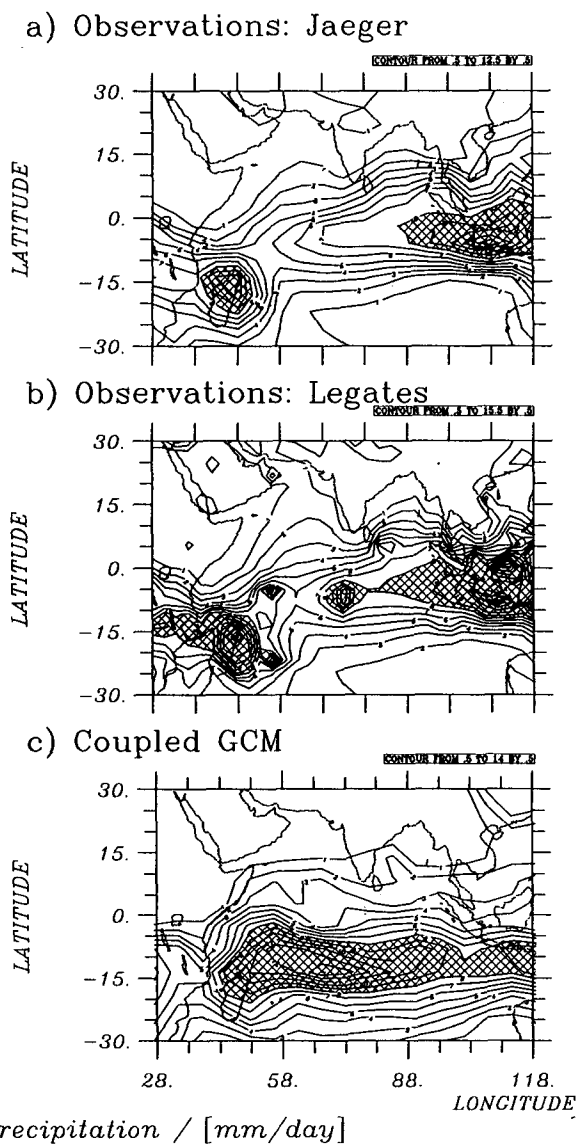

FIG. 3. (a) Climatological January rainfall (mm/day) after Jäger (1976) and (b) after Legates and Willmott (1990). (c) Long-term mean January rainfall (mm/day) derived from the 26-year run with the CGCM. Shading indicates rainfall of ≥ 8 mm/day.

so that the Somali Current is simulated much too weak by the coupled model attaining maximum speeds of only 50 cm s^{-1}, whereas observations indicate a strength of at least 100 cm s^{-1}. It should be noted, however, that a high-resolution version of the ocean component is capable of realistic simulations of the Indian Ocean circulation when forced by observed surface wind stresses (Villwock 1994, personal communication). Thus, the sluggish Somali Current arises primarily from the coarse model resolution.

The annual cycle in rainfall averaged over India and Burma is shown in Fig. 10. The coupled model simulates realistically the temporal evolution of the rainfall. The maximum rainfall, however, while simulated correctly during July, is only of the order of 250 mm/day (Fig. 10b), whereas the observations indicate a peak value of about 350 mm/day (Fig. 10a). This model failure can be attributed to the atmosphere model, which yields a similar result when forced by observed SSTs (not shown). In summary, the CGCM reproduces a reasonable annual cycle in the Indian Ocean/Asian region.

4. Interannual variability

Our coupled model simulates considerable variability on interannual timescales. This interannual variability, however, is mostly restricted to the Indian Ocean circulation. Typical spectra of atmospheric quantities, such as surface wind stress or heat flux over the equatorial Indian Ocean are white. Thus, to first order the low-frequency variability in the Indian Ocean circulation is consistent with the "stochastic climate model" idea of Hasselmann (1976), according to which the ocean integrates the atmospheric noise. Large-scale unstable air–sea interactions, as observed over the Pacific Ocean, are not simulated over the Indian Ocean by our CGCM.

a. Monsoon/ENSO linkage

One of the main questions regarding the interannual variability in the Indian Ocean/Asian region is its relationship to the ENSO phenomenon. Several studies suggest that ENSO originates over the Indian Ocean and then propagates slowly eastward into the Pacific region (e.g., Barnett 1983). We showed in Part I of this paper that, consistent with this idea and observations, our CGCM simulates a westerly wind stress anomaly over the northwestern Pacific prior to the extremes of the model ENSO. This feature could indicate a relationship of our model ENSO to the Indian Ocean region. We therefore investigated the relationship between the interannual variability in the Indian Ocean/Asian region to the ENSO phenomenon. We applied several different statistical techniques in order to investigate whether or not interannual variability in the Pacific is forced, at least occasionally, by processes outside the Pacific. None of the results indicate that the processes in the Indian Ocean/Asian region influence significantly the ENSO cycle in the Pacific. As hypothesized by Latif et al. (1993b), the occurrence of the westerly wind stress anomaly prior to the extremes of the ENSO cycle results from processes within the climate system over the Pacific itself and is due entirely to an anomalous meridional SST gradient near the equator.

b. Indian Ocean response to ENSO

We did find, however, a significant response of the Indian Ocean circulation to ENSO. This behavior is

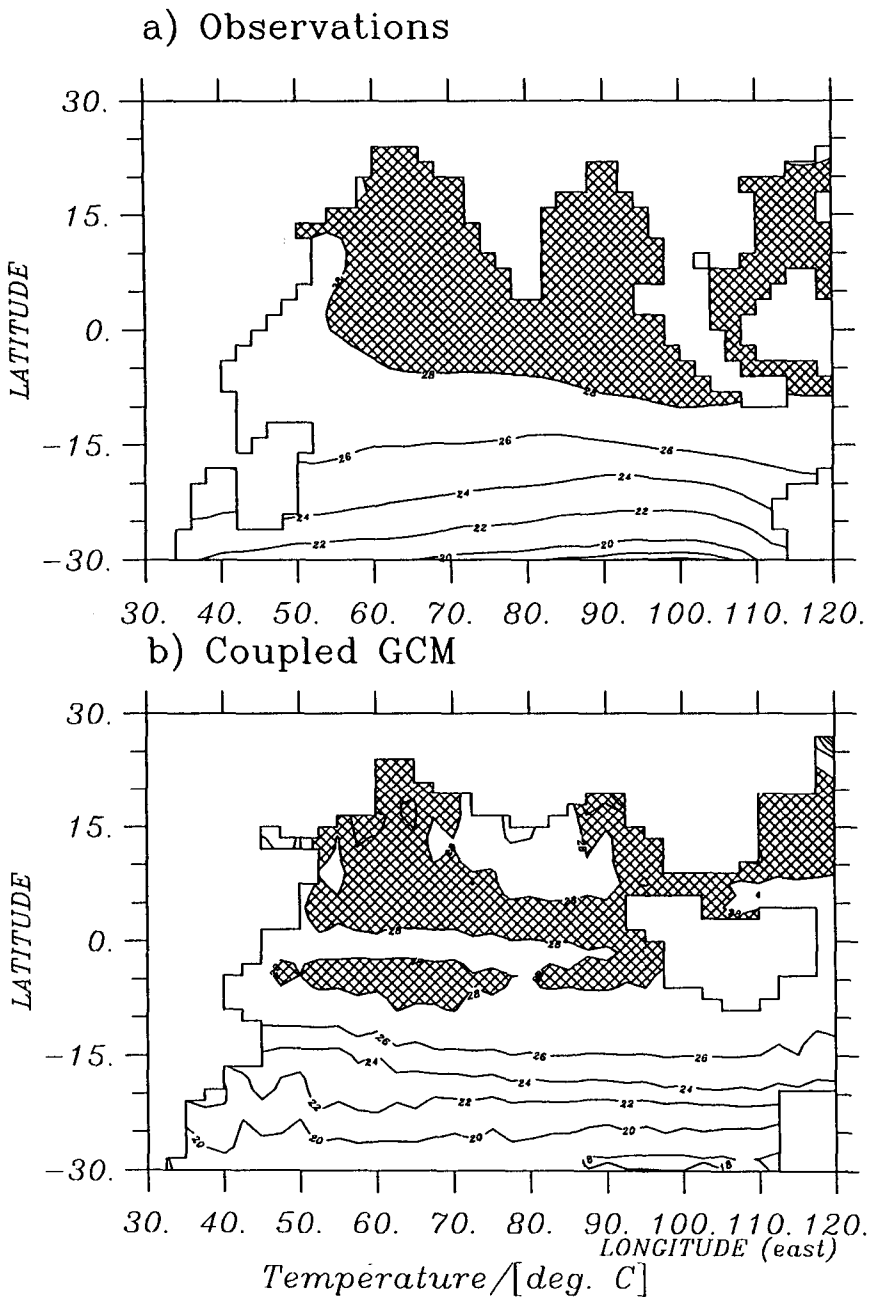

FIG. 4. (a) Climatological July SST (°C) after Levitus (1982); (b) long-term mean July SST (°C) derived from the 26-year run with the CGCM. Shading indicates areas with SST $\geq$ 28°C.

best seen in a cross-spectral analysis of eastern equatorial Pacific SST anomalies (commonly expressed by the Niño-3 index, an area average over the region 5°N–5°S, 150°W–90°W) and SST anomalies averaged over the central Indian Ocean (2°N–2°S, 70°E–90°E), which is presented in Fig. 11. As expected, the low-frequency variability in the Indian Ocean SST is about one order of magnitude less than that in the equatorial Pacific SST; this is clearly seen in the autospectra of the two time series (Fig. 11a). The squared coherence between the Indian Ocean and the Pacific SST anomalies (Fig. 11c) shows a pronounced maximum at a period of about 3 years, which is the preferred ENSO timescale in the CGCM (see Part I). The peak in the

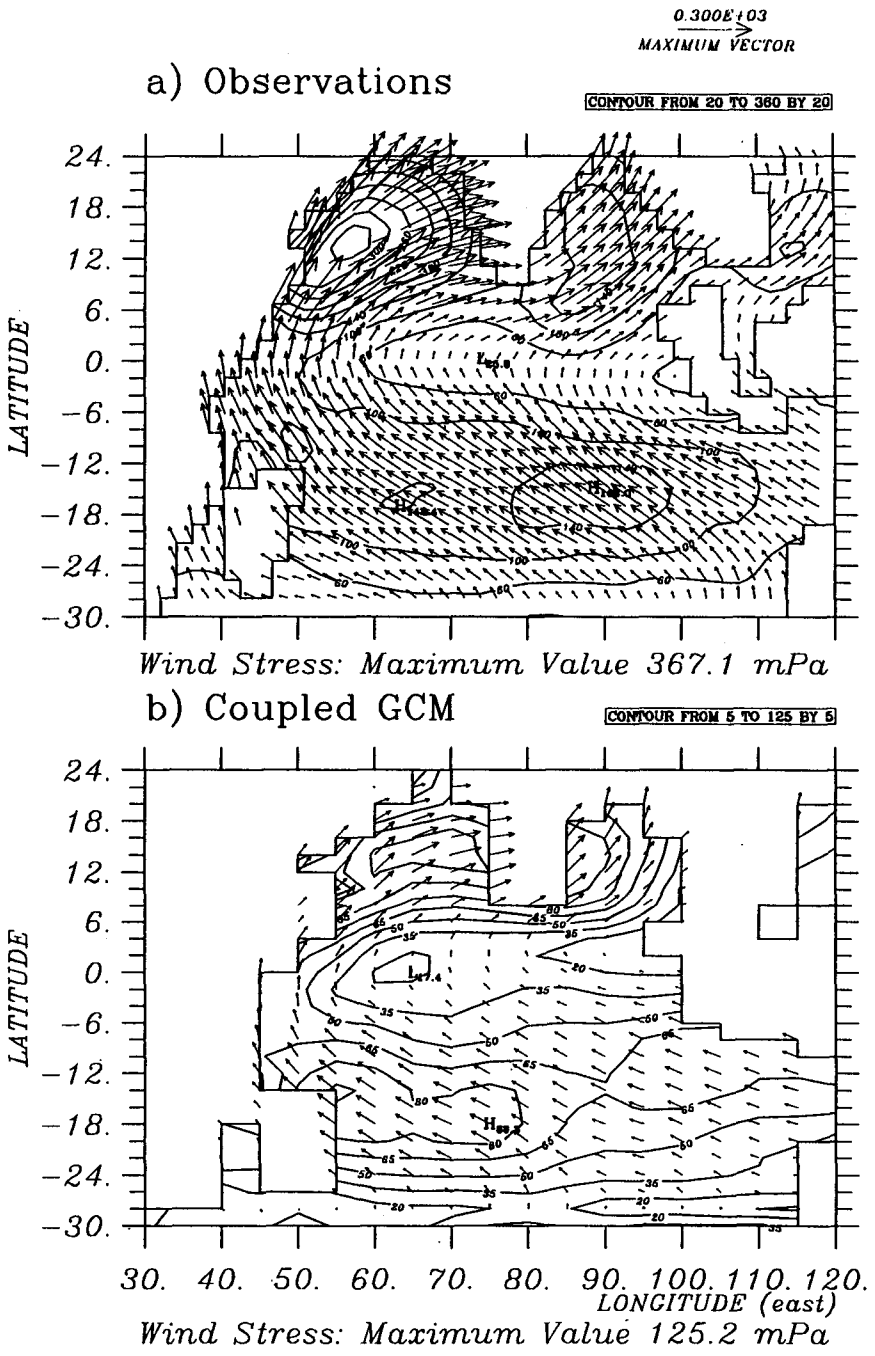

FIG. 5. (a) Climatological July surface wind stress (m Pa) after Hellermann and Rosenstein (1983); (b) long-term mean July surface wind stress (m Pa) derived from the 26-year run with the CGCM.

squared coherence is significant on the 99% significance level. The corresponding phase spectrum indicates a phase shift of about 45°, or 5 months, with the equatorial Pacific SST anomalies leading (Fig. 11b). This result is also confirmed by an ordinary cross-correlation analysis. Maximum cross correlation between the two time series is found also at a lag of 5 months. We note also that at very long timescales [O(10 yr)] the tropical Pacific and tropical Indian Ocean vary in phase.

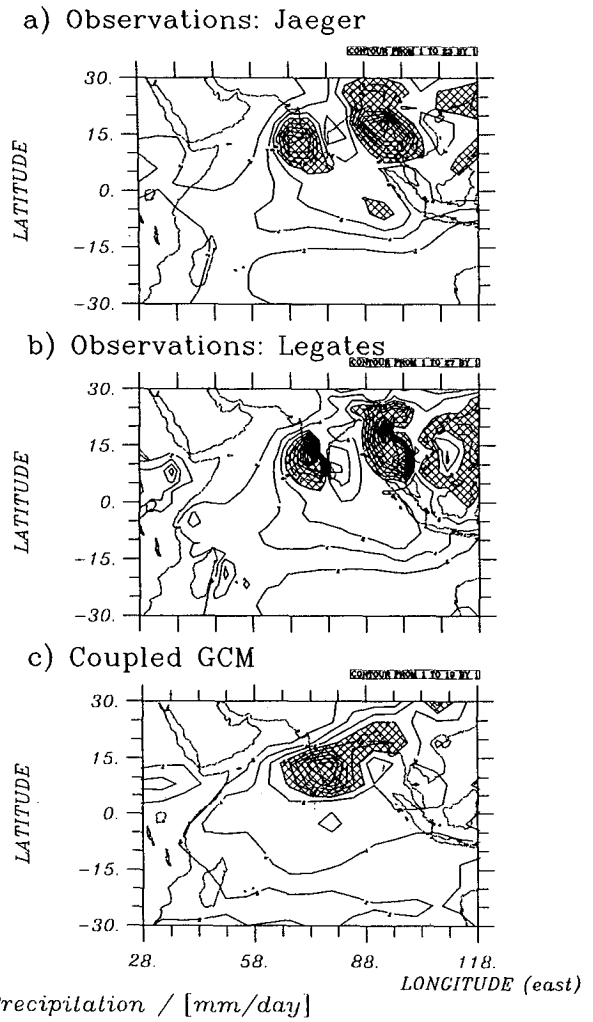

FIG. 6. (a) Climatological July rainfall (mm/day) after Jäger (1976) and (b) after Legates and Willmott (1990). (c) Long-term mean July rainfall (mm/day) derived from the 26-year run with the CGCM. Shading indicates rainfall of 8 mm/day and more.

In addition, we carried out cross-spectral analyses of the Niño-3 SST anomaly time series with equatorial Indian Ocean zonal wind stress anomalies and of equatorial Indian Ocean SST with zonal wind stress anomalies averaged over the same region. These two additional cross-spectral analyses show coherence peaks at a period of 3 years significant at the 99% and 95% level respectively (not shown). Furthermore, the corresponding phases at this period are consistent with the idea that low-frequency changes in the Indian Ocean circulation are forced by changes in the Pacific circulation. Thus, we conclude that in our coupled model the Indian Ocean responds *passively* to the interannual variability in the Pacific Ocean.

The physical processes involved in this response of the Indian Ocean SST to ENSO are similar to those responsible for ENSO itself. This can be seen from Fig. 12, which shows the associated patterns of (low-pass filtered) equatorial Indian Ocean zonal wind stress (Fig. 12a) and SST (Fig. 12b) anomalies to the Nino-3 timeseries. Positive SST anomalies in the central and

TABLE 1. Monsoon rainfall statistics derived from observations, the coupled general circulation model (CGCM), and the uncoupled atmospheric general circulation model (AGCM) forced by observed SSTs. Rainfall was averaged over India and Burma.

	Rainfall (mm)	Std dev (mm)	Std dev (%)
Observations	1067	137	13
CGCM	950	66	7
Uncoupled AGCM	932	76	8

TABLE 2. Statistics of the monsoon onset date derived from observations, the coupled general circulation model (CGCM), and the uncoupled atmospheric general circulation model (AGCM) forced by observed SSTs. Rainfall was averaged over India and Burma. The monsoon onset is defined as the data at which a rainfall of 3 mm/day is exceeded.

	Onset date	Std dev (days)
Observations	1 June	7.7
CGCM	3 June	6.4
Uncoupled AGCM	2 June	10.0

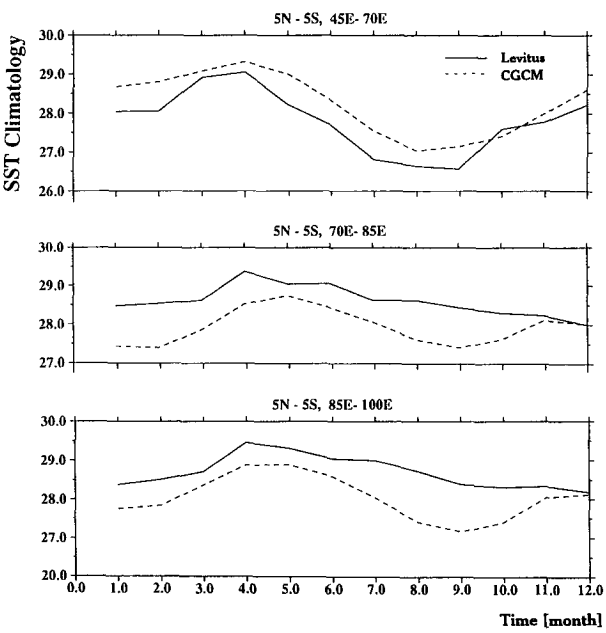

FIG. 7. Time series of climatological SST (°C) in three equatorial boxes as simulated by the coupled model (dashed lines) and as given by the Levitus climatology (full lines).

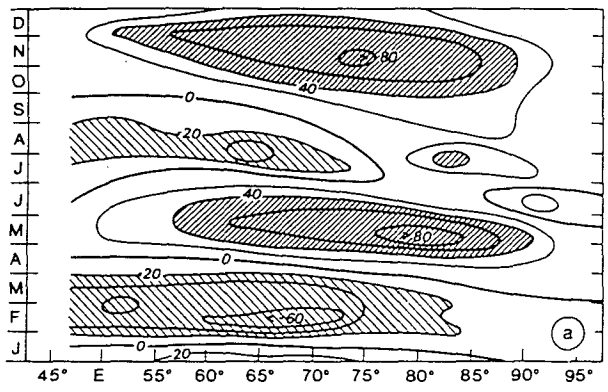

FIG. 8a. Hovmoeller diagram of climatological zonal surface currents (cm s^{-1}) at the equator [after Reverdin (1987)].

eastern Indian Ocean are forced by westerly wind stress anomalies. Furthermore, the associated pattern of surface heat flux anomalies (not shown) shows that the surface heat flux anomalies are out of phase with the SST anomalies so that the role of the surface heat flux is to damp the SST anomalies. Both relationships implied by our statistical analyses are found also in the Pacific (e.g., Barnett et al. 1991). The picture derived from the CGCM can be summarized as follows: Once a significant SST anomaly has developed in the eastern equatorial Pacific, anomalous westerly winds develop over the equatorial Pacific and the central and eastern equatorial Indian Ocean in response to an eastward

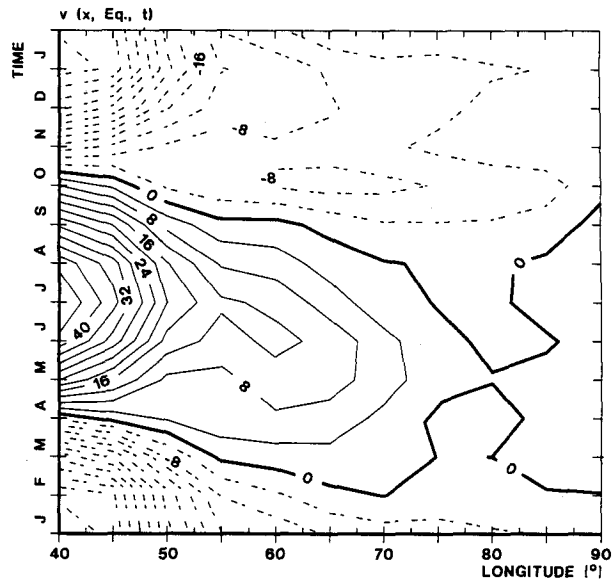

FIG. 9. Hovmoeller diagram of long-term mean meridional surface currents (cm s^{-1}) at the equator derived from the 26-year run with the CGCM.

shift of the rising branch of the Walker circulation (Fig. 12a). The westerly wind stress anomalies over the Indian Ocean are associated with anomalous downwelling that warms the ocean's surface (Fig. 12b). Horizontal advection is unlikely to be important because of the weak horizontal SST gradients in the equatorial Indian Ocean (Figs. 1 and 4).

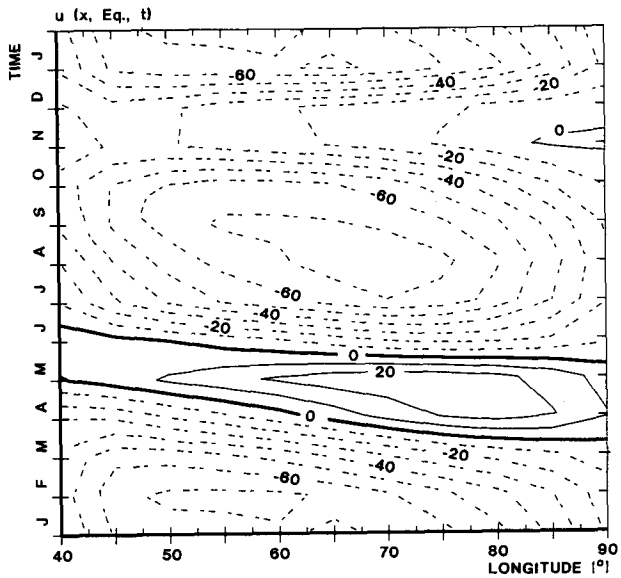

FIG. 8b. Hovmoeller diagram of long-term mean zonal surface currents (cm s^{-1}) at the equator derived from the 26-year run with the CGCM.

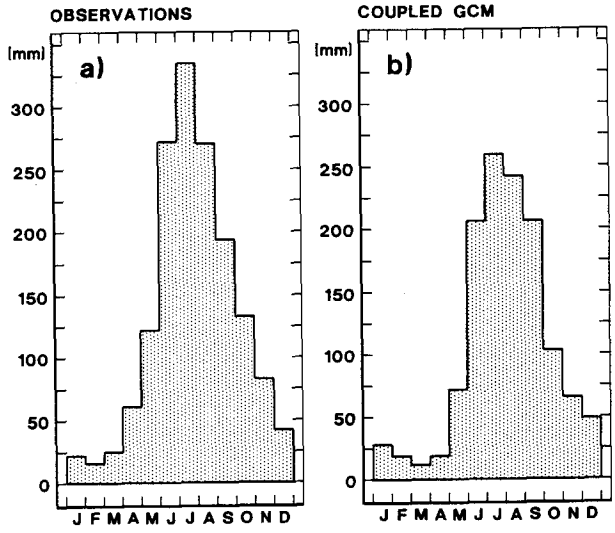

FIG. 10. (a) Climatological rainfall (mm/day) averaged over India and Burma as a function of calendar month after Jäger (1976); (b) long-term mean rainfall (mm/day) averaged over the same region and as a function of calendar month derived from the 26-year run with the CGCM.

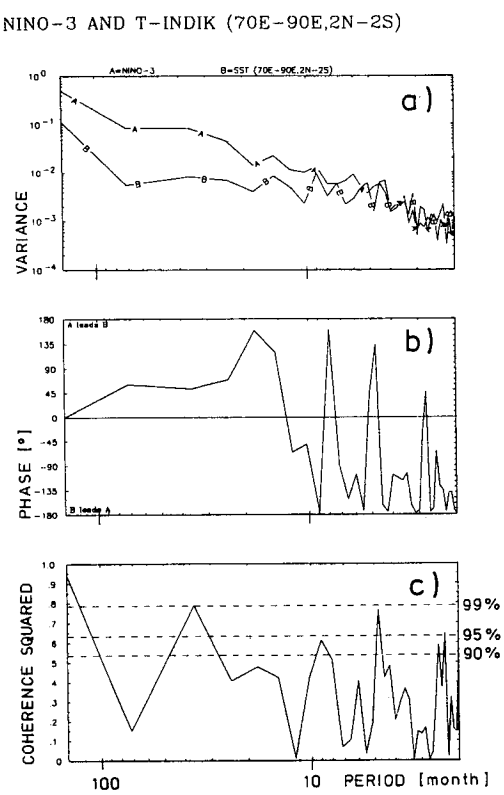

FIG. 11. Cross-spectral analysis of eastern equatorial Pacific SST anomalies in the Niño-3 region (an area average of equatorial Pacific SST anomalies over the region 5°N–5°S, 150°W–90°W) and central equatorial Indian Ocean SST anomalies. Upper panel: autospectra; middle panel: phase spectrum; lower panel: coherence spectrum.

c. *Interannual monsoon variability*

Evidence exists for the Indian summer monsoon rainfall to be below normal during El Niños when the SST in the Pacific is anomalously high and vice versa (Shukla 1990). We therefore investigate here whether our CGCM is able to simulate such a relationship, which would be important for successful monsoon rainfall predictions. We first investigated observational data and computed the cross-correlation between the Niño-3 SST anomaly timeseries and annual rainfall averaged over India and Burma. Two significant extremes in the cross-correlation function are found (Fig. 13a). Niño-3 SST anomalies are negatively correlated with the monsoon rainfall during and shortly after the monsoon season, which confirms the results of Shukla (1990). The second extreme in the cross-correlation function indicates that eastern equatorial SST anomalies in the fall prior to the monsoon season are positively correlated with the rainfall anomalies during the monsoon season. Although the physical mechanisms leading to this lead–lag relationship between Niño-3 SST and rainfall anomalies are still controversial, the statistical relationship itself is well established.

We then computed the cross-correlation function of monsoon rainfall and Niño-3 SST anomalies from the output of our CGCM. The coupled model does not show any significant relationship between the two quantities (Fig. 13b). This behavior explains why the monsoon variability in the CGCM is considerably weaker than observed (Table 1). The model failure, however, does not affect the variability in the onset date, which is reasonably well simulated by the CGCM (Table 2) and is probably related to internal processes within the atmosphere itself, such as the 30–60 day oscillation (Madden and Julian 1972).

The question then arises whether the lack of sufficient interannual variability in monsoon rainfall is related to climate drift of the coupled model. In particular, the western equatorial Pacific cooled significantly during the course of the coupled integration (see Part I, Fig. 1), which could reduce deep convection and the impact of El Niño on the global atmospheric circulation. In order to answer this question, we computed the cross-correlation function for a stand-alone integration with our AGCM in which it was forced by observed near-global SSTs for the period 1970–1988 [details of this run can be found in Latif et al. (1990) and Barnett et al. (1991)]. No consistent lead–lag relationship between monsoon rainfall and tropical Pacific SST was found in this run either (Fig. 13c). Thus, either important physical processes that relate changes in SST to changes in monsoon rainfall (such as surface land processes) are not parameterized adequately in our atmosphere model or, due to insufficient resolution, changes in the large-scale atmospheric circulation are not reflected in the rainfall. At this stage, we cannot give a satisfactory explanation for the model failure. Further experiments are under way to investigate this issue in more detail.

5. Conclusions

We have analyzed the annual cycle and interannual variability in the Indian Ocean/Asian region simulated by a coupled ocean–atmosphere general circulation model in an integration of 26-years duration. We draw the following main conclusions from this study.

1) The CGCM simulates realistically the annual cycle in key parameters, such as Indian Ocean SST or monsoon rainfall. This, however, applies to gross indices only. Regional details are not well simulated by the CGCM.

2) The Indian Ocean responds passively to the ENSO-related interannual variability in the tropical Pacific. SST anomalies of the same sign as those in the Pacific are simulated in the Indian Ocean several months after SST anomalies peak in the Pacific.

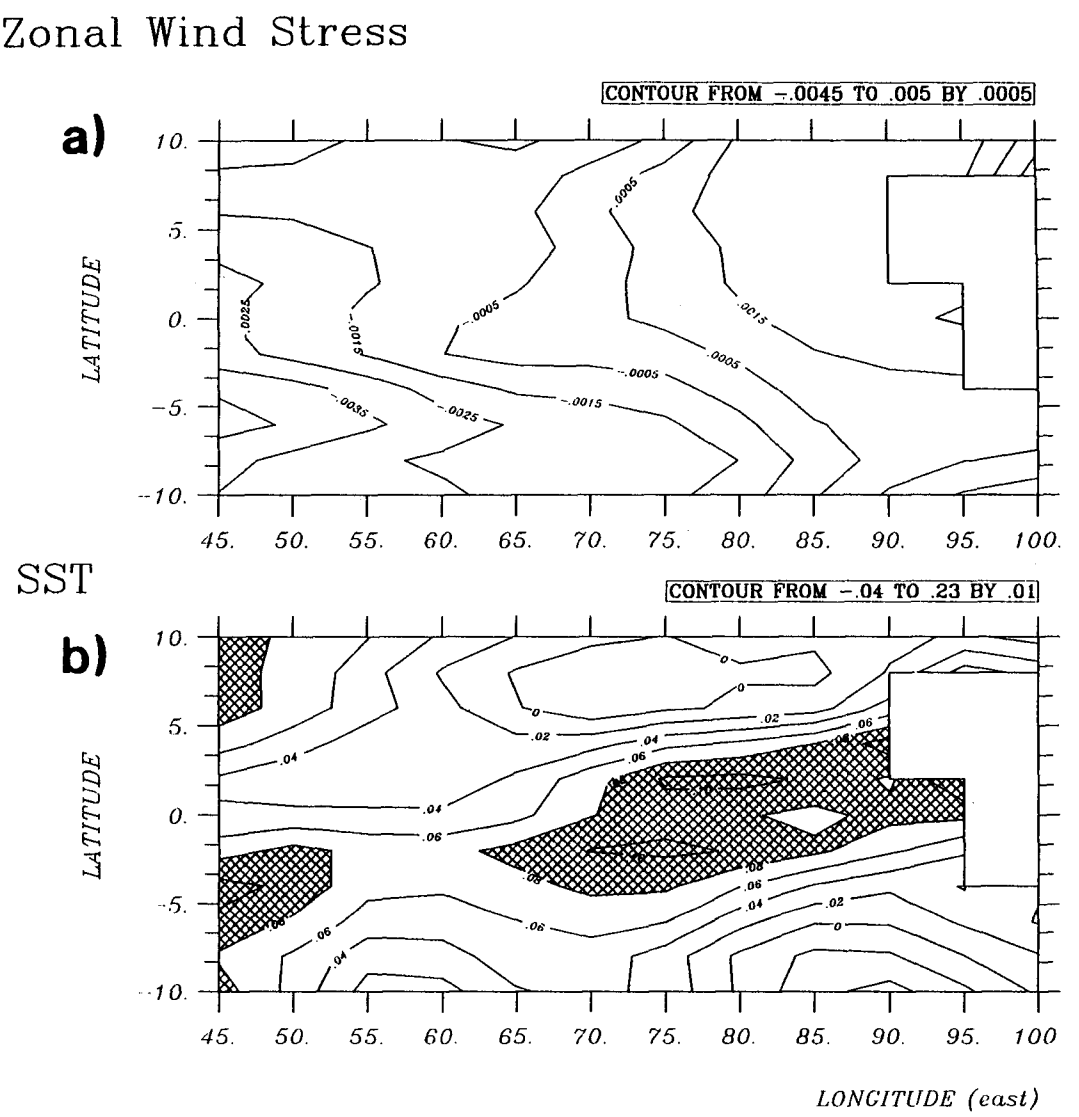

FIG. 12. Associated pattern of (a) equatorial Indian Ocean zonal wind stress (Pa) and (b) SST anomalies (°C) to the Niño-3 time series. The patterns show the anomalies corresponding to one standard deviation change in the Niño-3 time series. Shading indicates SST anomalies ≥ 0.08°C.

3) The physical processes involved in this response of the Indian Ocean circulation are related to anomalous upwelling. The surface heat flux acts as a negative feedback.

4) The CGCM fails to simulate sufficient interannual variability in monsoon rainfall. This failure can be traced back to the atmosphere model, which does not respond correctly to SST anomalies. Therefore, monsoon predictions with our CGCM appear premature.

Our coupled integration shows positive and negative aspects in both the ocean and atmosphere. Encouraging, for instance, is that the coupled model reproduces the annual cycle in area-averaged monsoon rainfall (Fig. 10) and the mean monsoon onset date and its variability. The coupled model also simulates reasonably well area-averaged Indian Ocean SST and the annual reversal of the Somali Current (Fig. 9). On the other hand, the coupled model fails to simulate sufficient interannual variability in monsoon rainfall and its correct relationship to the ENSO phenomenon (Fig. 13) or the correct strength of the Indian Ocean surface currents. Some of the problems might be reduced by using higher resolution, but our results suggest also that some of the parameterizations of physical processes in ocean and atmosphere might be flawed or not optimally tuned. Thus, much work remains to be

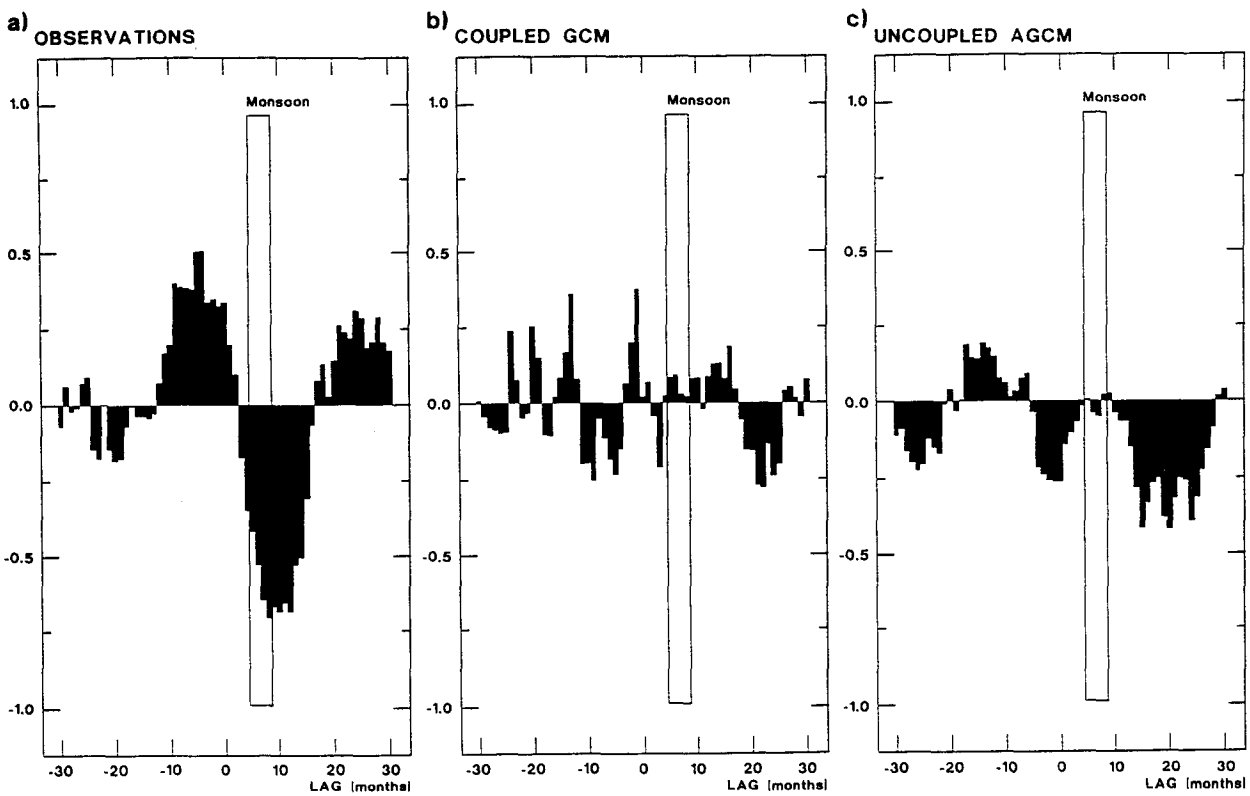

FIG. 13. Cross correlation function of Niño-3 SST anomalies with annual rainfall averaged over India and Burma as derived from (a) observations, (b) the 26-year run with the CGCM, and (c) an uncoupled run with the AGCM forced by global observed SSTs. The time lag is in months and the bar indicates the monsoon season.

done until coupled models will realistically simulate the patterns of climate variability in the Indian Ocean–Asian region.

Acknowledgments. We would like to thank Dr. Klaus Arpe, Dr. Erich Roeckner, and Mr. Andreas Villwock for many fruitful discussions. Many thanks also to Mrs. Marion Grunert for preparing the diagrams. This work was supported by the European Community under Contract EV5V-CT92-0121 and by the Koerber Project. The integrations were carried out at the Deutsches Klimarechenzentrum (DKRZ).

REFERENCES

Barnett, T. P., 1983: Interaction of the monsoon and Pacific trade wind system at interannual time scales. Part I: The equatorial zone. *Mon. Wea. Rev.*, **111**, 756–773.

——, L. Dümenil, U. Schlese, E. Roeckner, and M. Latif, 1989: The effect of Eurasian snow cover on regional and global climate. *J. Atmos. Sci.*, **46**, 661–685.

——, M. Latif, E. Kirk, and E. Roeckner, 1991: On ENSO physics. *J. Climate*, **4**, 487–515.

Hahn, D. J., and J. Shukla, 1976: An apparent relationship between Eurasian snow cover and Indian monsoon rainfall. *J. Atmos. Sci.*, **33**, 2461–2462.

Hasselmann, K., 1976: Stochastic climate models. Part I: Theory. *Tellus*, **28**, 473–485.

Hellerman, S., and M. Rosenstein, 1983: Normal monthly wind stress over the world ocean with error estimates. *J. Phys. Oceanogr.*, **13**, 1093–1104.

Jäger, L., 1976: Monatskarten des Niederschlages für die ganze Erde. *Ber. Dtsch. Wetterdienstes*, **139**, 1–38.

Knox, R. A., 1987: The Indian Ocean: Interactions with the monsoons. *Monsoons*, J. Fein and P. Stephens, Eds., J. Wiley and Sons, 365–398.

——, and D. L. T. Anderson, 1985: Recent advances in the study of low-latitude ocean circulation. *Progress in Oceanography*, Vol 14, Pergamon, 259–318.

Latif, M., J. Biercamp, H. von Storch, M. J. McPhaden, and E. Kirk, 1990: Simulation of ENSO related surface wind anomalies with an atmospheric GCM forced by observed SST. *J. Climate*, **3**, 509–521.

——, A. Sterl, E. Maier-Reimer, and M. M. Junge: 1993a: Climate variability in a coupled GCM. Part I: The tropical Pacific. *J. Climate*, **6**, 5–21.

——, ——, ——, and ——, 1993b: Structure and predictability of the El Niño/Southern Oscillation phenomenon in a coupled ocean–atmosphere general circulation model. *J. Climate*, **6**, 700–708.

Legates, D. R., and C. J. Willmott, 1990: Mean seasonal and spatial variability in gauge corrected global precipitation. *J. Climatol.*, **10**, 111–127.

Levitus, S., 1982: *Climatological Atlas of the World Ocean.* NOAA Prof. Paper No. 13, U.S. Govt. Printing Office, Washington, D.C., 173 pp, 17 microfiche.

Lighthill, M. J., 1969: Dynamic response of the Indian Ocean to onset of the Southwest Monsoon. *Philos. Trans. Roy. Soc. London,* Ser. A, **265,** 45–92.

Luther, M. E., 1987: Indian Ocean modeling. *Further Progress in Oceanography,* E. Katz and J. Witte, Eds., Nova University Press, 303–316.

Madden, R. A., and P. R. Julian, 1972: Description of global-scale circulation cells in the tropics with a 40–50 day period. *J. Atmos. Sci.,* **29,** 1109–1123.

Meehl, G. A., 1989: The coupled ocean–atmosphere modeling problem in the tropical Pacific and Asian monsoon regions. *J. Climate,* **2,** 1146–1163.

——, 1992: Effect of tropical topography on global climate. *Annu. Rev. Earth Planet. Sci.,* **20,** 85–112.

Neelin, J. D., and Co-authors, 1992: Tropical air–sea interaction in general circulation models. *Climate Dyn.,* **7,** 73–104.

Reverdin, G., 1987: The upper equatorial Indian Ocean: The climatological seasonal cycle. *J. Phys. Oceanogr.,* **17,** 903–927.

Shukla, J., 1990: Short term climate variability and predictions. Conference volume, *Second World Climate Conf.,* Geneva, Switzerland, WMO. [Available from World Meteorological Organization, Case Postale No. 2300, CH-1211 Geneva 20, Switzerland.]

WMO, 1992: Simulation of interannual and intraseasonal monsoon variability. Report of workshop, National Center for Atmospheric Research, Boulder, Colorado, U.S.A., 21.–24. October, 1992. World Climate Research Programme, WCRP-68, WMO/TD No. 470. [Available from World Meteorological Organization, Case Postale No. 2300, CH-1211 Geneva 20, Switzerland.]

Wyrtki, K., 1973: An equatorial jet in the Indian Ocean. *Science,* **181,** 262–264.